DALTON
FULL PAPER

Structure and vibrational properties of ethyltrioxorhenium(VII), $C_2H_5ReO_3$, investigated by gas electron diffraction, single crystal X-ray diffraction, IR spectroscopy and quantum chemical calculations †

Anthony J. Downs,*[a] Martin R. Geisberger,[b] Jennifer C. Green,[a] Tim M. Greene,*[c] Arne Haaland,*[d] Wolfgang A. Herrmann,[b] Leigh J. Morris,[a] Simon Parsons,*[e] Wolfgang Scherer*[b] and Hans Vidar Volden[d]

[a] *Inorganic Chemistry Laboratory, University of Oxford, South Parks Road, Oxford, UK OX1 3QR. E-mail: tony.downs@chem.ox.ac.uk*
[b] *Anorganisch-chemisches Institut, Technische Universität München, Lichtenbergstrasse 4, D-85747 Garching bei München, Germany*
[c] *School of Chemistry, University of Exeter, Stocker Road, Exeter, UK EX4 4QD*
[d] *Department of Chemistry, University of Oslo, Box 1033, Blindern, N-0315 Oslo, Norway*
[e] *Department of Chemistry, University of Edinburgh, West Mains Road, Edinburgh, UK EH9 3JJ*

Received 1st May 2002, Accepted 2nd July 2002
First published as an Advance Article on the web 8th August 2002

The electron diffraction pattern of gaseous ethyltrioxorhenium(VII) has been analysed in terms of a $C_2H_5ReO_3$ molecule with C_s symmetry overall. Least-squares refinement yields the following dimensions (r_a in Å, angles in deg): Re–C 2.095(6), C–C 1.530(16), Re–O 1.711(2), C–H 1.106(13), Re–C–C 112.0(9), and O–Re–C 104.6(5). The compound forms monoclinic crystals [$a = 6.421(3)$, $b = 5.111(2)$, $c = 15.108(5)$ Å; $\beta = 98.01(4)°$ at 150 K] composed of discrete molecules little different dimensionally from the gaseous species. Both the structure and IR spectrum of the molecule isolated in an Ar matrix are well reproduced by density functional theory (DFT) calculations. There is no hint of anything unusual about the geometry of the C_2H_5Re fragment, but the C–C–Re skeleton is appreciably stiffer to bending at the C_α atom than is the C–C–Ti skeleton in the titanium compound $C_2H_5TiCl_3$.

The discovery that methyltrioxorhenium(VII), CH_3ReO_3, is an efficient catalyst in a wide range of organic reactions[1,2] and the ensuing investigations of its reactivity and physical properties[3] have naturally stimulated interest in its higher alkyl homologues. Thus, it was in 1991 that Herrmann *et al.* succeeded in isolating a sample of the ethyl analogue $C_2H_5ReO_3$, **1**, from the reaction of Re_2O_7 with $(C_2H_5)_2Zn$ in THF at −78 °C.[4] With a melting point of −21 °C, the compound is a colourless, relatively volatile liquid that is immune to attack by air and moisture at ambient temperatures. The thermal stability is also unusual, decomposition setting in only slowly at 60 °C and probably proceeding *via* $C_2H_5^{\bullet}$ radical formation as a result of Re–C bond homolysis, rather than β-hydrogen elimination.[4] Accordingly, the compound was greeted as the first example of a thermally stable alkyloxo-transition metal complex containing β-hydrogen atoms. Although the catalytic potential has not been explored to the same extent as has that of the methyl derivative, ethyltrioxorhenium can act as a catalyst, for example in the epoxidation of alkenes or oxidation of aromatic molecules by H_2O_2.[5]

The IR spectrum of **1** in the solid and solution states has been analysed on the basis of a molecular model with a staggered $H_3C–CH_2Re$ moiety and C_s symmetry overall,[6] but no definitive structural studies have been carried out hitherto. With a relatively electron-rich metal centre, there is no reason to expect the ethyl ligand to be perturbed by so-called 'agostic' interactions [as in $CH_3CH_2TiCl_3(Me_2PC_2H_4PMe_2)$, for example].[7,8] However, the unusual structure and evidence of tilted methyl groups in the related compound trimethyldioxorhenium, $(CH_3)_3ReO_2$,[9] suggest that delocalisation giving the appearance of C–H ··· Re interactions is by no means impossible in these rhenium(VII) species with a valence electron count at, or close to, 18.

Here we report the results of gas electron diffraction (GED) studies carried out on the vapour of **1** and also of X-ray diffraction studies carried out on single crystals of the compound grown at low temperature. These reveal the presence of discrete $CH_3CH_2ReO_3$ molecules with an undistorted ethyl group and dimensions that are not perceptibly affected by the transition from the gaseous to the crystalline state. Both the structure and vibrational properties of the molecule are well reproduced by density functional theory (DFT) calculations. The one major difference between **1** and the ethyltitanium compound $CH_3CH_2TiCl_3$[8] is the force constant defining the bending of the $M–C_\alpha–C_\beta$ unit which is nearly twice as big for **1** (M = Re) as it is for the titanium compound. The greater rigidity of the CH_3CH_2Re fragment must be attributed, at least in part, to a less polar M–C interaction in **1**.

Experimental

Synthesis

Ethyltrioxorhenium(VII), **1**, was synthesised in THF in its normal and perdeuteriated forms by the reaction of Re_2O_7

† Electronic supplementary information (ESI) available: details of the calculations, including vibrational properties and cartesian coordinates of the optimised geometries of $ReO_3C_2D_5$ and $ReO_3C_2H_5$. See http://www.rsc.org/suppdata/dt/b2/b204235p/

 DOI: 10.1039/b204235p

(Aldrich, 99.9+%) with $Zn(C_2H_5)_2$ and $Zn(C_2D_5)_2$, respectively (prepared by heating C_2H_5I or C_2D_5I with a Zn/Cu mixture),[10] according to the method described previously.[4] The black residue left after evaporation of the solvent at −5 °C was extracted with pentane at −20 °C. Cooling of the pale yellow extract to −78 °C afforded colourless crystals of **1**: any remaining solvent was evaporated *in vacuo* at −40 °C. **1** was authenticated by its IR spectrum, typically measured for a thin film of the annealed condensate formed at 77 K.[6]

DFT calculations

DFT calculations have been carried out at two levels. The first set (DFT1) employed the Gaussian 94 program system.[11] The geometry was optimised at the BPW91 level of density functional theory. A quasi-relativistic effective-core potential (ECP) and [8s6p3d]/(3s2p2d) basis from Hay and Wadt[12] was used for Re in conjunction with Dunning bases[13] on C, O and H. The second, more recent set (DFT2) employed the ADF 2000 program suite.[14,15] The electronic configuration of the $C_2H_5ReO_3$ molecule was described by an uncontracted triple-ζ basis set of Slater-type orbitals (STO), carbon and oxygen being given extra (3d) polarisation functions. The cores of the atoms were frozen, C and O up to 1s, Re up to 4d, and relativistic corrections were made to the cores of all atoms using the ZORA formalism. In both the DFT1 and DFT2 sets, energies were calculated using Vosko, Wilk and Nusair's local exchange correlation potential,[16] with non-local exchange corrections by Becke,[17] and non-local correlation corrections by Perdew,[18] while vibrational wavenumbers were computed by numerical differentiation of slightly displaced geometries.[19] Further details concerning the vibrational calculations, along with the cartesian coordinates of the optimised geometry, are available as ESI.

IR spectra of matrix-isolated 1 and 1-d_5

The vapour of **1** or **1**-d_5 held at 256 K was codeposited continuously with an excess of Ar on a CsI window cooled to 16 K by means of a Displex closed-cycle refrigerator (Air Products Model CS 202); fuller details of the apparatus are given elsewhere.[20] Typical deposition rates were *ca.* 3 mmol of matrix gas per hour, continued over a period of 2 h. IR spectra of the matrix samples were recorded with a Nicolet 'Magna' 560 FT-IR spectrometer over the range 4000–400 cm^{-1} at a resolution of 0.5 cm^{-1} and with a wavenumber accuracy of ±0.1 cm^{-1}.

GED measurements and structure refinements

Electron-diffraction measurements on the vapour of **1** were carried out with the Balzers KDG-2 unit at Oslo,[21] with the sample reservoir at 268 K and the vapour being injected in the dark *via* an all-glass inlet system held at room temperature. Exposures were made at nozzle-to-plate distances of *ca.* 50 cm (6 plates) and 25 cm (5 plates). The plates were traced using a modified Joyce-Loeb1 microdensitometer, and the data processed with a program written by T. G. Strand (University of Oslo). Atomic scattering factors were taken from ref. 22. Backgrounds were drawn as least-squares-adjusted polynomials to the difference between the total experimental and the calculated molecular scattering intensities. Least-squares refinements were carried out with the program KCED26 written by G. Gundersen, S. Samdal, H. M. Seip, and T. G. Strand (University of Oslo).

Structure refinements by least-squares calculations on the GED data were based on a molecular model with C_s symmetry overall and a staggered conformation of the CH_3CH_2Re unit, as indicated in Fig. 1. In the light of the results of the DFT calculations (*q.v.*), the $CReO_3$ fragment was modelled on the assumption of local C_{3v} symmetry; a common C–H bond distance and a methyl group with local C_{3v} symmetry were also assumed. The geometry of the methylene group was defined by C_s symmetry with the restriction that the CH_2 plane bisects the ReCC angle. In addition, identical H–C–H angles were assumed in the CH_3 and CH_2 groups. The molecular structure was then determined by seven independent geometrical parameters, *viz.* the bond distances Re–C, Re–O, C–C, and C–H, and the valence angles ∠CReO, ∠ReCC, and ∠CCH(methyl). Initial refinements were performed without corrections for thermal vibrations. Inclusion of vibrational correction terms ($D = r_\alpha - r_a$) led to a slightly improved fit but to no significant changes of the estimated geometrical parameters. Refinement of the CCH (methyl) angle led finally to a value of 110° but with a relatively large standard deviation of 4°.

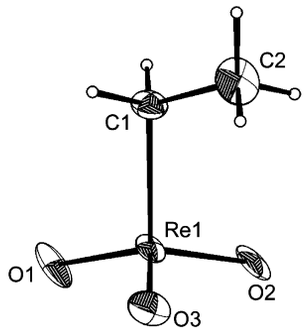

Fig. 1 Structure of $C_2H_5ReO_3$, **1**, in the solid state; ellipsoids enclose 50% probability surfaces (see ref. 27).

The DFT1 force field of **1** was used to calculate the root-mean-square (rms) vibrational amplitudes, vibrational correction terms, *D*, and force constants by means of the program ASYM20.[23] A single scale factor (0.94) for the theoretical force field was optimised by minimising the rms deviations between the calculated and observed wavenumbers. The C–C amplitude, which could not be refined satisfactorily on the basis of the GED results, was fixed at the calculated value of 0.053 Å in the final stages of refinement.

Crystal growth and crystallography of 1 at 150 K

A liquid sample of **1** was sealed under vacuum in a preconditioned thin-walled Pyrex glass capillary 2.5–3.0 cm in length; warming to room temperature gave a column of liquid 1.0–1.5 cm in depth. Single crystals were grown by careful cooling following earlier precedents.[24] The capillary was fixed to a goniometric head and mounted in the cold stream of an Oxford Cryosystems low-temperature device[25] attached to a Stoë Stadi four-circle diffractometer. A stable solid–liquid phase boundary was established within the sample at 262.5 K, and crystallisation induced by cooling at approximately 20 K h^{-1}. The diffraction pattern was indexed using the program DIRAX.[26] X-Ray data were collected with the crystal at 150 K.

Details of the crystal data and data collection are given in Table 1. An optimised numerical absorption correction was made by refining an approximately cylindrical morphology against ψ-scan data (Stoë X-Shape).[28] Of the 5095 reflections measured, 1422 were independent (R_{int} = 0.0734); of these 658 had $F > 4\sigma(F)$. The structure was solved by direct methods (SIR92)[29] and refined by full-matrix least squares against *F* (CRYSTALS).[30] H atoms were placed in calculated positions and the non-H atoms were modelled with anisotropic displacement parameters. The refinement converged to $R = 4.06\%$, and $R_w = 4.35\%$ using a Carruthers–Watkin weighting scheme.[31] The final difference map extremes were +2.51 and −2.68 e $Å^{-3}$.

CCDC reference number 185060.

See http://www.rsc.org/suppdata/dt/b2/b204235p/ for crystallographic data in CIF or other electronic format.

Table 1 Crystal data, data collection and structure refinement for ethyltrioxorhenium, **1**, at 150 K

Empirical formula	$C_2H_5ReO_3$
Formula weight	263.26
Crystal system	Monoclinic
Space group	$P2_1/n$
a/Å	6.421(3)
b/Å	5.111(2)
c/Å	15.108(5)
β/°	98.01(4)
Volume/Å^3	491.0(5)
Z	4
Density (calc.)/Mg m^{-3}	3.56
Absorption coefficient/mm^{-1}	24.97
Reflections collected	5095
Independent reflections	1422 (R_{int} 0.0734)
Conventional R [$F > 4\sigma(F)$]	R_1 0.0406 (658 data)
Weighted R (F^2 and all data)	0.0435

Results and discussion

DFT calculations

The optimised geometry established by the DFT2 calculations for $C_2H_5ReO_3$ approximates closely to that determined crystallographically and illustrated in Fig. 1. As expected, this geometry features a staggered CH_3CH_2Re unit. The Re–C and C–C distances are calculated to be 2.100 and 1.534 Å, respectively, the Re–O distances are all equal within less than 0.001 Å at 1.725 Å, and the C–H distances are also equal within 0.0025 Å, with a mean value of 1.100 Å (see Table 4). The $CReO_3$ framework approximates closely to regular C_{3v} symmetry with ∠O–Re–O and ∠O–Re–C averaging 113.0 and 105.7°, respectively. The $ReCH_2CH_3$ fragment is characterised by ∠Re–C–C = 113.3° and ∠H–C–H(mean) = 107.9° (with deviations not exceeding 0.3°). There is a slight tilting of the CH_3 group with respect to the C–C directrix, ∠C–C–H for the H atom *trans* to the metal atom being about 2° smaller than the other two. Although this effect lies beyond the scope of recognition of the present GED studies, it is almost certainly real and reflects the unsymmetrical character of the torsional potential created by the CH_2Re unit with respect to the CH_3 rotor. Tilt angles between 0.8 and 1.5° in the same direction have certainly been found, on the evidence of microwave studies, in the halogeno derivatives CH_3CH_2Cl,[32] CH_3CH_2Br,[33] and CH_3CH_2I.[34] Far from appearing to be attracted towards the metal centre through agostic interactions, as in $[C_2H_5TiCl_3(dmpe)]$ (dmpe = $Me_2PCH_2CH_2PMe_2$),[8] then, the β-CH_3 group actually shows signs of weak repulsion from the ReO_3 portion of the molecule. Such repulsion is evident too in the somewhat enlarged value of 113.3° calculated for the Re–C–C valence angle, although the effect is not as pronounced as in the free $CH_3CH_2TiCl_3$ molecule where ∠Ti–C–C = *ca.* 117°.[8]

The energy of a $C_2H_5ReO_3$ molecule with C_s symmetry but with the C_2H_5Re group locked in an *eclipsed* conformation was calculated (DFT1) to be 7.9 kJ mol^{-1} higher than that of the equilibrium structure. The implied barrier to rotation about the C–C bond is thus marginally greater than that in $C_2H_5TiCl_3$ (7.1 kJ mol^{-1}) as calculated at a similar level of theory.

The IR spectra of **1** and its perdeuteriated isotopomer **1**-d_5 have been calculated (DFT2) in their optimised geometries. How well theory simulates the vibrational properties, as well as the structures, of these molecules will now be revealed.

IR spectra

The IR spectrum of **1** has been described previously[6] only for the condensed phases where the effects of intermolecular forces may result in significant perturbation of the molecules. The volatility of the compound is not sufficient to allow more than a very limited number of IR transitions to be observed for the vapour at ambient temperatures; moreover, rotational broadening of the absorptions impairs the resolution of near-degenerate transitions. To overcome these problems, we have turned to the IR spectra of **1** and **1**-d_5 each isolated at high dilution in a solid Ar matrix. Illustrated in Fig. 2 beneath the calculated spectrum is the IR spectrum of a matrix sample of **1**; relevant details of both the measured and calculated spectra are listed, together with the proposed assignments, in Table 2.

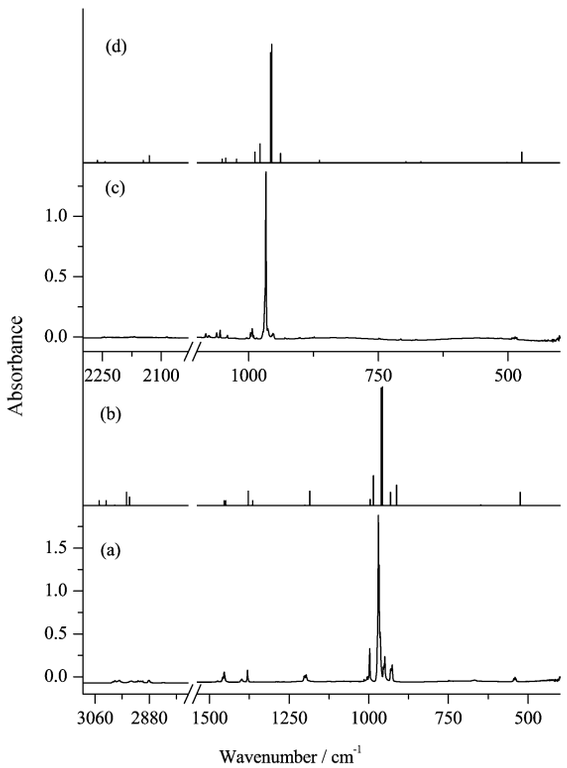

Fig. 2 (a) IR spectrum of $C_2H_5ReO_3$, **1**, isolated in an argon matrix at 16 K. (b) IR spectrum calculated for **1**. (c) IR spectrum of $C_2D_5ReO_3$, **1**-d_5, isolated in an argon matrix at 16 K. (d) IR spectrum calculated for **1**-d_5.

While displaying much sharper bands and significantly more detail, the matrix spectrum of **1** resembles closely the spectra of the compound in the solid and solution states.[6] Hence there is every reason to believe that the essentially discrete $CH_3CH_2ReO_3$ molecule is preserved in the condensed as well as the vapour phases, and that intermolecular forces are relatively weak (in keeping with the volatility of the compound). The 27 vibrational fundamentals are distributed under the C_s symmetry calculated for the molecule over the representations 16a′ + 11a″, and the calculations also lead us to expect that 19 of these fundamentals occur in the wavenumber range 4000–400 cm^{-1} spanned by the present experiments.

The measured matrix spectra have been analysed and assignments made on the basis of three principal criteria: (i) the response of a particular band to the effects of deuteriation; (ii) comparison with the spectra forecast by the DFT calculations; and (iii) comparison with the results of earlier studies involving both **1**[6] and CH_3ReO_3.[35] The spectra are complicated in places by what we take to be the effects of matrix-splitting, as displayed, for example, in the spectrum of **1** by the weak absorption near 540 cm^{-1} attributable to the ν(Re–C) mode. The most intense absorption, occurring at 970.1/967.4 cm^{-1} in the spectrum of **1** and suffering only a slight shift on deuteriation, is plainly associated with the antisymmetric $\nu(ReO_3)$ modes, with the symmetric counterpart appearing at 997.3 cm^{-1}. The relative intensities of these two features appear[35] to confirm that ∠O–Re–O is in the order of 110°. Additional distinctive features of **1** are the weak absorptions between 2880 and 3000 cm^{-1} associated with the ν(C–H) fundamentals,

Table 2 Observed and calculated vibrational wavenumbers for $C_2H_5ReO_3$ [a]

$C_2H_5ReO_3$		$C_2D_5ReO_3$		
Obs.	Calc.[b]	Obs.	Calc.[b]	Description
2994.6/2980.3 (9)	3045.8 (4)	2245.2/2227.5 (3)	2263.1 (2)	ν(C–H)
2939.6 (3)	3023.0 (4)	2170.4 (2)	2243.4 (1)	
[c]	2994.2 (0.1)	2125.6 (1)	2225.0 (0.01)	
2916.8/2909.2/2901.6 (14)	2955.3 (11)	2112.5 (1)	2145.6 (2)	
2881.7 (4)	2945.6 (7)	2086.3 (2)	2130.1 (6)	
1458.3/1454.0 (9)	1453.6 (4)	1054.3 (2)	1051.1 (3)	$\delta_{as}(CH_3)$
	1448.7 (4)	1041.0 (1)	1044.0 (4)	
1380.6 (5)	1378.2 (12)	[c]	987.6 (9)	$\delta(CH_2)$
1361.5 (0.04)	1364.5 (4)	[c]	1023.2 (3)	$\delta_s(CH_3)$
1203.3/1200.1/1196.6 (9)	1200.4 (0.1)	873.6 (1)	863.2 (2)	CH_2 wag
	1185.0 (12)	[c]		
1005.0 (2)	995.7 (5)	[c]	938.5 (8)	ν(C–C)
997.3 (12)	985.3 (25)	996.4 (9)	978.0 (16)	$\nu_s(ReO_3)$
970.1/967.4 (100)	960.5 (99)	967.0 (100)	957.6 (93)	$\nu_{as}(ReO_3)$
	956.8 (100)	[c]	955.4 (100)	
949.9 (15)	931.7 (11)	708.6 (1)	696.9 (1)	$\delta(C_2H_5)$
926.7 (12)	912.8 (17)	678.1 (1)	668.1 (1)	CH_2 twist
[c]	648.4 (0.6)	514.3 (1)	502.0 (0.3)	$\rho(CH_2)$
544.3/540.7/537.8 (4)	524.5 (11)	489.3/485.9 (3)	473.5(9)	ν(Re–C)

[a] Wavenumbers in cm^{-1}; intensities in parentheses, normalised to that of the most intense band set equal to 100. [b] Values taken from DFT2 calculations; for details see text. [c] Feature that is obscured or too weak to be observed.

Table 3 Comparison of the principal force constants in selected ethyl compounds

	Force constant/N m^{-1}			
Molecule	E–C stretching[a]	C–C stretching	E–C–C bending[a]	Ref.
C_2H_5Cl	323.9	445.3	95.7	36
C_2H_5Br	244.9	456.1	98.9	37
C_2H_5I	191.0	422.6	94.1	38
$(C_2H_5)_2Zn$	242[b]	354[b]	70[b]	39
$C_2H_5ReO_3$	235.2	401.9	49.8	This work
$C_2H_5TiCl_3$	180.9	404.1	28.2	8

[a] E = Cl, Br, I, Zn, Re or Ti. [b] Based on an approximate force field.

and others at 1005.0, 949.9 and 926.7 cm^{-1} attributable to the ν(C–C), $\delta(C_2H_5)$, and CH_2 twist motions, respectively.

How well the DFT calculations reproduce the IR spectra observed for matrix-isolated **1** and **1**-d_5 is shown by the stick diagram included in Fig. 2 and also by the results detailed in Table 2, with an rms deviation for 30 wavenumbers of only 1.87%. This must give us considerable confidence in the ability of the DFT methods we have used to model the properties of **1**. Selected force constants derived from the scaled force field are given in Table 3, together with the corresponding parameters for other ethyl compounds, *viz.* C_2H_5Cl,[36] C_2H_5Br,[37] C_2H_5I,[38] and $C_2H_5TiCl_3$.[8] Compared with the titanium compound, there is a significant increase in the M–C stretching force constant in **1** consistent with a metal–carbon bond that is not only stronger but also less polar. On the other hand, compared with its methyl analogue, CH_3ReO_3, for which f(M–C) = 264.9 N m^{-1},[6] **1** shows an 11% decrease in f(M–C), suggesting a weakening of the metal–carbon bond in the ethyl derivative. More striking still in the comparison between $C_2H_5TiCl_3$ and $C_2H_5ReO_3$ is the reduced pliability of the C_2H_5Re moiety with respect to bending at the C_α atom, the relevant bending force constant showing a 77% increase on that for the titanium compound.

GED analysis

The final structure refinements by least-squares analysis of the experimental GED data yielded the structure parameters and vibrational amplitudes contained in Table 4. Experimental and calculated molecular scattering curves are depicted in Fig. 3a, the corresponding radial distribution curves in Fig. 3b. Refinements were also carried out with a C_s model having an *eclipsed* CH_3CH_2Re group. These resulted in marginally poorer agreement between experimental and calculated intensities, but the difference was too small to rule out the eclipsed conformation on the basis of the GED measurements alone. Significantly, though, the value determined for the ReCC angle was independent of the conformation assumed by the C_2H_5Re group.

There is, as revealed in Table 4, generally very satisfactory agreement between the experimentally determined and DFT-calculated structures. Only one of the primary dimensions has an experimental value that differs by more than three standard deviations from the calculated one. The one exception is the Re–O distance, than which no parameter is better defined experimentally, and so the difference of 0.014 Å (or 7 standard deviations) between the experimental and calculated estimates must reflect theoretical deficiencies. Otherwise, the experimental results provide impressive endorsement of all the structural details anticipated by the calculations. This includes the somewhat enlarged Re–C–C valence angle, confirming that there is not so much attraction as *repulsion* between the β-methyl group and the O atoms of the ReO_3 substrate in *gauche* positions.

Table 4 Interatomic distances, valence angles, rms vibrational amplitudes (l) and vibrational correction terms (D) in $C_2H_5ReO_3$ determined by gas electron diffraction (GED) and DFT calculations, and compared with the corresponding geometrical parameters determined by X-ray diffraction measurements on a single crystal at 150 K [a]

	Gaseous molecule, GED and DFT results						
Parameter	r_a(GED)	r_e(DFT1) [b]	r_e(DFT2) [b]	l(GED)	l(DFT1) [b]	D(DFT1) [b]	Single crystal at 150 K
Bond distances							
Re–C	2.095(6)	2.078	2.100	4.5(5)	5.3	−0.3	2.098(14)
C–C	1.530(16)	1.548	1.534	[5.3] [c]	5.3	−2.2	1.510(2)
Re–O	1.711(2)	1.742	1.725	3.1(2)	3.6	−0.6	1.671(11), 1.702(12), 1.707(11)
C–H	1.106(13)	1.105 [d]	1.100 [d]	12.6(14)	7.8	−4.4	1.00(2)
Non-bonded distances							
Re ··· C_β	3.008(16)	3.041	3.051	8.0(13)	9.2	−0.6	2.97(2)
O ··· O	2.864(7)	2.910 [d]	2.877 [d]	7.1(13)	7.6	−0.6	2.83(3)
O ··· C_α	3.016(11)	3.045 [d]	3.057 [d]	8.4(17)	10.1	−0.2	3.02(2)
O ··· C_β(*cis*)	3.444(24)	3.518	3.524	17.5(28)	20.6	0.5	3.38(2), 3.44(2)
O ··· C_β(*trans*)	4.338(18)	4.421	4.423	9.9(35)	9.1	−0.1	4.312(19)
Valence angles							
∠Re–C_α–C_β	112.0(9)	113.2	113.3	—	—	—	109.8(11)
∠O–Re–C_α	104.6(5)	105.3 [d]	105.7 [d]	—	—	—	105.8(6), 104.5(5), 104.6(5)

[a] Distances, vibrational amplitudes and correction terms in Å, angles in deg. Estimated standard deviations in parentheses in units of the last digit. As the GED refinements were carried out with diagonal weight matrices, the esds have been doubled to include an estimated scale uncertainty of 0.1%. *R*-factors: GED 0.022 (50 cm), 0.07 (25 cm), 0.045 (total); X-ray R_1 0.0406. [b] See text. [c] Value in square brackets was unrefined. [d] Average values. Individual distances and angles (DFT2) are: C–H(methyl) 1.098, 1.097, 1.101; C–H(methylene) 1.102, 1.102; O ··· O 2.875, 2.876, 2.879; O ··· C_α 3.049, 3.053, 3.069; ∠O–Re–C_α 105.3, 105.5, 106.3.

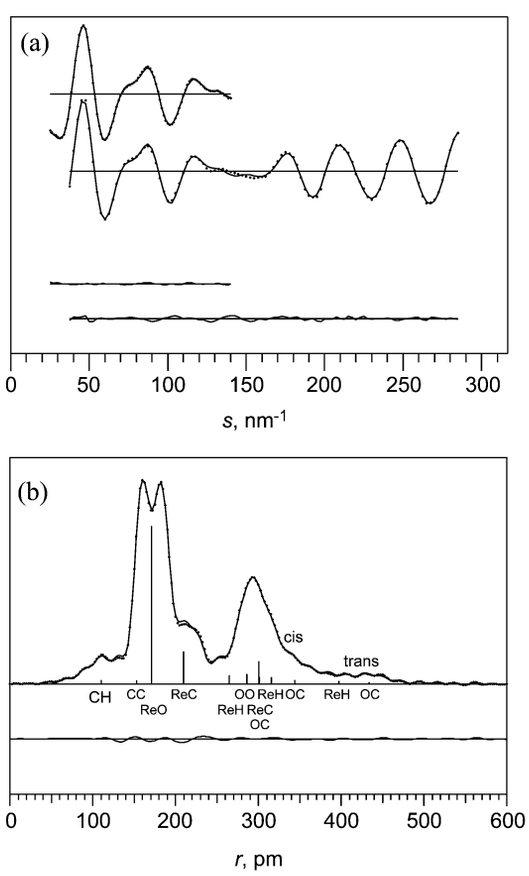

Fig. 3 (a) Top: experimental (dots) and calculated (line) molecular scattering curves for gaseous **1**. Below: difference curves. (b) Top: experimental (dots) and calculated (line) modified radial distribution curves for **1**. Below: difference curve. Artificial damping constant $k = 25$ pm^2. The structural refinements are based on the molecular model described in the text.

Table 5 compares the primary dimensions of **1** with those of CH_3ReO_3,[3] as well as CH_3TiCl_3,[39] $C_2H_5TiCl_3$,[8] $(C_2H_5)_2Zn$,[40] and C_2H_5X (X = Cl,[32] Br,[33] or I[34]) as determined for the gaseous molecules. Hence it is evident that the M–C bond distances in the ethyl compounds $C_2H_5ReO_3$ and $C_2H_5TiCl_3$ are about 0.04 Å longer than in the methyl analogues. This too suggests a weakening of the metal–carbon bonds in the ethyl compounds. Circumstantial support comes from the Zn–C bond distance which is 0.02 Å longer in $(C_2H_5)_2Zn$ than in $(CH_3)_2Zn$ according to GED measurements,[40] while the Zn–C bond dissociation energy is reported to be 42 kJ mol^{-1} smaller in the ethyl compound.[41] A similar but substantially smaller effect is displayed by the carbon–halogen bonds in C_2H_5X (X = Cl,[32] Br,[33] or I[34]) which are about 0.01 Å longer than in the corresponding CH_3X molecules. Experiment and theory are agreed that the C–C–X angle in the halogenoethane molecules is close to 111°,[32–34,36] *i.e.* marginally greater than the tetrahedral value, but distinctly narrower than the comparable angles in $C_2H_5ReO_3$ (*ca.* 113°), $(C_2H_5)_2Zn$ (114.5°),[40] and $C_2H_5TiCl_3$ (*ca.* 117°).[8] As in CH_3ReO_3,[3] the ReO_3 pyramid of $C_2H_5ReO_3$ is somewhat flattened to give C–Re–O and O–Re–O angles of 104.6(5) and 113.9(4)°, respectively [*cf.* 106.0(2) and 112.7(2)° in CH_3ReO_3].

Crystal structure

The structure of crystalline **1** at 150 K, illustrated in Fig. 4, consists of more or less discrete $C_2H_5ReO_3$ molecules with the same geometry as in the gas phase. Table 4 includes the relevant intramolecular dimensions. The molecules are packed in strands with long intermolecular Re ··· O contacts measuring 3.414(12) and 3.522(11) Å engaging two of the O atoms of each molecule. This has the effect of producing one short bond distance of 1.671(11) Å for the Re–O bond that does not enter into these interactions, and two longer ones averaging 1.705(12) Å. Hence the intermolecular interactions are plainly quite weak. The only other parameter to show a difference exceeding 1 standard deviation is the Re–C–C angle which appears to be narrower in the crystalline than in the vapour state, but even this is not statistically significant. In short, the molecule suffers no appreciable change of dimensions with the switch from the vapour to the crystal, and the ethyl group shows no sign of significant secondary interaction, whether intra- or intermolecular in nature.

Conclusions

The present quantum chemical, IR, GED and X-ray diffraction studies provide the first definitive structural characterisation of

Table 5 Comparison of the structures of gaseous $C_2H_5ReO_3$, CH_3ReO_3, and other ethyl and methyl derivatives (distances in Å, angles in deg)

Molecule	r(E–C)[a]	r(E–X)[a]	r(C–H)	∠C–E–X[a]	∠E–C–C[a]	Ref.
CH_3ReO_3[b]	2.060(9)	1.709(3)	1.105(12)	106.0(2)	—	3
$C_2H_5ReO_3$[b]	2.095(6)	1.711(2)	1.106(13)	104.6(5)	112.0(9)	This work
CH_3TiCl_3[b]	2.047(6)	2.185(3)	1.098(6)	105.6(2)	—	39
$C_2H_5TiCl_3$[b]	2.090(15)	2.195(3)	1.104(10)	104.6(4)	116.6(11)	8
$(C_2H_5)_2Zn$[b]	1.950(2)	1.950(2)	1.105(4)	180	114.5(3)	40
C_2H_5Cl[c]	1.789(1)	—	1.089(1)[d]	—	111.0(1)	32
C_2H_5Br[c]	1.950(1)	—	1.087(1)[d]	—	111.0(1)	33
			1.092(1)[e]			
C_2H_5I[c]	2.151(1)	—	1.086(1)[d]	—	111.6(1)	34
			1.093(1)[e]			

[a] E = Re, Ti, Zn, Cl, Br or I; X = O, Cl or C. [b] r_a structure determined by GED measurements. [c] r_s structure determined by microwave measurements. [d] CH_2 group. [e] CH_3 group.

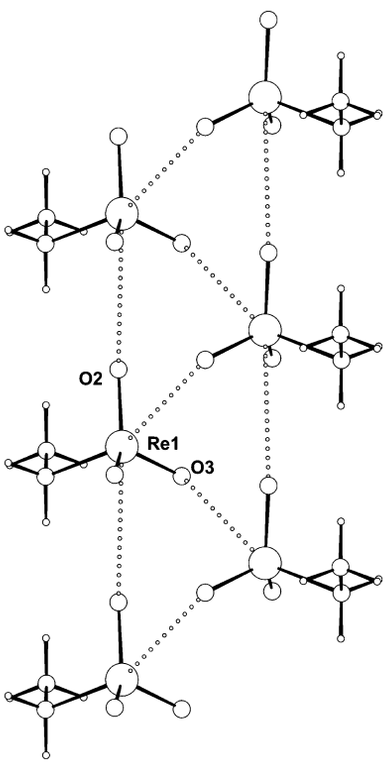

Fig. 4 Intermolecular contacts in the crystal structure of $C_2H_5ReO_3$, **1**. The view is perpendicular to (001), with [010] running vertically (see ref. 27).

ethyltrioxorhenium, **1**, in both the vapour and crystalline states. DFT calculations anticipate well both the geometry and vibrational properties of the gaseous $CH_3CH_2ReO_3$ molecule, as revealed by the GED pattern of the vapour and the IR spectra of the isotopically natural and perdeuteriated molecules isolated in Ar matrices. The dimensions are similar to those of other ethyl compounds; the CH_3CH_2Re unit adopts, as expected, a staggered conformation with an Re–C–C angle about 2° wider than those in C_2H_5X molecules (X = Cl, Br, or I),[32–34] but rather narrower than those in $(C_2H_5)_2Zn$[40] and $C_2H_5TiCl_3$.[8] Hence weak repulsion between the β-CH_3 and ReO_3 groups is indicated, with no hint of an agostic interaction. The vibrational force field is characterised by an Re–C–C bending force constant intermediate between those of C_2H_5X[36–38] and $C_2H_5TiCl_3$,[8] so that the potential surface defined by Re–C–C bending is shallower than in C_2H_5X but steeper than in $C_2H_5TiCl_3$. On the evidence of both the Re–C distance and the Re–C stretching force constant, there is a weakening of the Re–C bond when the CH_3 ligand in CH_3ReO_3 gives way to C_2H_5. Crystallisation of **1** preserves the $C_2H_5ReO_3$ molecules with only minor perturbations of the geometry resulting from weak secondary Re–O ··· Re interactions, but no suggestion of specific intermolecular interactions involving the C_2H_5 group.

Very recent studies have shown that isomerisation of matrix-isolated CH_3ReO_3 occurs under the action of broad-band UV-visible light to give the methylidene tautomer $H_2C{=}Re(O)_2OH$.[35] How **1** responds to photolysis under similar conditions and whether tautomerisation or β-hydrogen elimination ensues will be the subject of a separate paper.[42]

Acknowledgements

We are indebted (i) to the EPSRC for financial support of the Oxford group, an Advanced Fellowship (T. M. G.) and a studentship (L. J. M.), (ii) to the Deutsche Forschungsgemeinschaft for a postdoctoral fellowship (W. S.), (iii) to the VISTA program of STATOIL and the Norwegian Academy of Science and Letters for financial support, and (iii) to the Research Council of Norway for a generous grant of computing time.

References

1 W. A. Herrmann, *J. Organomet. Chem.*, 1995, **500**, 149.
2 C. C. Romão, F. E. Kühn and W. A. Herrmann, *Chem. Rev.*, 1997, **97**, 3197.
3 W. A. Herrmann, P. Kiprof, K. Rypdal, J. Tremmel, R. Blom, R. Alberto, J. Behm, R. W. Albach, H. Bock, B. Solouki, J. Mink, D. Lichtenberger and N. E. Gruhn, *J. Am. Chem. Soc.*, 1991, **113**, 6527; W. A. Herrmann, W. Scherer, R. W. Fischer, J. Blümel, M. Kleine, W. Mertin, R. Gruehn, J. Mink, H. Boysen, C. C. Wilson, R. M. Ibberson, L. Bachmann and M. Mattner, *J. Am. Chem. Soc.*, 1995, **117**, 3231.
4 W. A. Herrmann, C. C. Romão, R. W. Fischer, P. Kiprof and C. de Méric de Bellefon, *Angew. Chem., Int. Ed. Engl.*, 1991, **30**, 185.
5 W. Scherer, unpublished work.
6 J. Mink, G. Keresztury, A. Stirling and W. A. Herrmann, *Spectrochim. Acta*, 1994, **50A**, 2039.
7 M. Brookhart and M. L. H. Green, *J. Organomet. Chem.*, 1983, **250**, 395; M. Brookhart, M. L. H. Green and L.-L. Wong, *Prog. Inorg. Chem.*, 1988, **36**, 1.
8 (*a*) W. Scherer, T. Priermeier, A. Haaland, H. V. Volden, G. S. McGrady, A. J. Downs, R. Boese and D. Bläser, *Organometallics*, 1998, **17**, 4406; (*b*) A. Haaland, W. Scherer, K. Ruud, G. S. McGrady, A. J. Downs and O. Swang, *J. Am. Chem. Soc.*, 1998, **120**, 3762; (*c*) W. Scherer, W. Hieringer, M. Spiegler, P. Sirsch, G. S. McGrady, A. J. Downs, A. Haaland and B. Pedersen, *Chem. Commun.*, 1998, 2471; (*d*) D. C. McKean, G. S. McGrady, A. J. Downs, W. Scherer and A. Haaland, *Phys. Chem. Chem. Phys.*, 2001, **3**, 2781.
9 A. Haaland, W. Scherer, H. V. Volden, H. P. Verne, O. Gropen, G. S. McGrady, A. J. Downs, G. Dierker, W. A. Herrmann, P. W. Roesky and M. R. Geisberger, *Organometallics*, 2000, **19**, 22.
10 N. K. Hota and C. J. Willis, *J. Organomet. Chem.*, 1967, **9**, 169.
11 M. J. Frisch, G. W. Trucks, H. B. Schlegel, P. M. W. Gill, B. G. Johnson, M. A. Robb, J. R. Cheeseman, T. Keith, G. A. Petersson, J. A. Montgomery, K. Raghavachari, M. A. Al-Laham, V. G. Zakrzewski, J. V. Ortiz, J. B. Foresman, J. Cioslowski, B. B. Stefanov, A. Nanayakkara, M. Challacombe, C. Y. Peng, P. Y. Ayala, W. Chen,

M. W. Wong, J. L. Andres, E. S. Replogle, R. Gomperts, R. L. Martin, D. J. Fox, J. S. Binkley, D. J. Defries, J. Baker, J. P. Stewart, M. Head-Gordon, C. Gonzales and J. A. Pople, Gaussian 94, Revision C.2, Gaussian Inc., Pittsburgh, PA, 1995.
12 P. J. Hay and W. R. Wadt, *J. Chem. Phys.*, 1985, **82**, 270, 299.
13 T. H. Dunning, *J. Chem. Phys.*, 1971, **55**, 716.
14 E. J. Baerends, A. Berces, C. Bo, P. M. Boerringter, L. Cavallo, L. Deng, R. M. Dickson, D. E. Ellis, L. Fan, T. H. Fischer, C. Fonseca Guerra, S. J. van Gisbergen, J. A. Groeneveld, O. V. Gritsenko, F. E. Harris, P. van den Hoek, H. Jacobsen, G. van Kessel, F. Kootstra, E. van Lenthe, V. P. Osinga, P. H. T. Philipsen, D. Post, C. C. Pye, W. Ravenek, P. Ros, P. R. T. Schipper, G. Schreckenbach, J. G. Snijider, M. Sola, D. Swerhone, G. te Velde, P. Vernooijs, L. Versluis, O. Visser, E. van Wezenbeek, G. Wiesenekker, S. K. Wolff, T. K. Woo and T. Ziegler, *ADF Program System Release 2000*, 1999.
15 G. Fonseca Guerra, J. G. Snijider, G. te Velde and E. J. Baerends, *Theor. Chim. Acta*, 1998, **99**, 391.
16 S. H. Vosko, L. Wilk and M. Nusair, *Can. J. Phys.*, 1980, **58**, 1200.
17 A. D. Becke, *Phys. Rev. A*, 1988, **38**, 3098.
18 J. P. Perdew, *Phys. Rev. B*, 1986, **33**, 8822.
19 L. Y. Fan and T. Ziegler, *J. Chem. Phys.*, 1992, **96**, 6937, 9005.
20 H.-J. Himmel, A. J. Downs, T. M. Greene and L. Andrews, *Organometallics*, 2000, **19**, 1060.
21 (*a*) W. Zeil, J. Haase and L. Wegmann, *Z. Instrumentenk.*, 1966, **74**, 84; (*b*) O. Bastiansen, R. Graber and L. Wegmann, *Balzers High Vac. Rep.*, 1969, **25**, 1.
22 A. W. Ross, M. Fink and R. Hilderbrandt, *International Tables for Crystallography*, ed. A. J. C. Wilson, Kluwer Academic Publishers, Dordrecht, 1992, Vol. C, p. 245.
23 L. Hedberg and I. M. Mills, *J. Mol. Spectrosc.*, 1993, **160**, 117.
24 C. Y. Tang, R. A. Coxall, A. J. Downs, T. M. Greene and S. Parsons, *J. Chem. Soc., Dalton Trans.*, 2001, 2141.
25 J. Cosier and A. M. Glazer, *J. Appl. Crystallogr.*, 1986, **19**, 105.
26 A. J. M. Duisenberg, *J. Appl. Crystallogr.*, 1992, **25**, 92.
27 D. J. Watkin, L. Pearce and C. K. Prout, Chemical Crystallography Laboratory, University of Oxford, 1993.
28 X-SHAPE, Stoë and Cie, Darmstadt, Germany, 1995.
29 A. Altomare, G. Cascarano, C. Giacovazzo and A. Guagliardi, *J. Appl. Crystallogr.*, 1993, **26**, 343.
30 D. J. Watkin, C. K. Prout, J. R. Carruthers, P. W. Betteridge and R. I. Cooper, CRYSTALS Issue 11.80, Chemical Crystallography Laboratory, University of Oxford, UK, 2002.
31 J. R. Carruthers and D. J. Watkin, *Acta Crystallogr., Sect. A*, 1979, **35**, 698.
32 M. Hayashi and T. Inagusa, *J. Mol. Struct.*, 1990, **220**, 103.
33 T. Inagusa and M. Hayashi, *J. Mol. Spectrosc.*, 1988, **129**, 160.
34 T. Inagusa, M. Fujitake and M. Hayashi, *J. Mol. Spectrosc.*, 1988, **128**, 456.
35 L. J. Morris, A. J. Downs, T. M. Greene, G. S. McGrady, W. A. Herrmann, P. Sirsch, W. Scherer and O. Gropen, *Organometallics*, 2001, **20**, 2344.
36 D. C. McKean, G. P. McQuillan, A. H. J. Robertson, W. F. Murphy, V. S. Mastryukov and J. E. Boggs, *J. Phys. Chem.*, 1995, **99**, 8994 and references cited therein.
37 S. Suzuki, J. L. Bribes and R. Gaufrès, *J. Mol. Spectrosc.*, 1973, **47**, 118.
38 G. A. Crowder, *J. Mol. Spectrosc.*, 1973, **48**, 467.
39 P. Briant, J. Green, A. Haaland, H. Møllendal, K. Rypdal and J. Tremmel, *J. Am. Chem. Soc.*, 1989, **111**, 3434.
40 A. Almenningen, T. U. Helgaker, A. Haaland and S. Samdal, *Acta Chem. Scand., Ser. A*, 1982, **36**, 159.
41 G. Pilcher and H. A. Skinner, *The Chemistry of the Metal-Carbon Bond*, ed. F. R. Hartley and S. Patai, Wiley, New York, 1982, p. 43.
42 L. J. Morris, J. C. Green, T. M. Greene and A. J. Downs, manuscript in preparation.